Food Packaging and Shelf Life 36 (2023) 101054

Contents lists available at ScienceDirect

Food Packaging and Shelf Life

journal homepage: www.elsevier.com/locate/fpsl

Effect of crystallinity on the migration of plastic additives from polylactic acid-based food contact plastics

Noémi Petrovics [a,b], Csaba Kirchkeszner [a,b], Antónia Patkó [b], Tamás Tábi [c,d], Norbert Magyar [e], Ilona Kovácsné Székely [e], Bálint Sámuel Szabó [a,b], Zoltán Nyiri [b], Zsuzsanna Eke [b,f,*]

[a] Hevesy György PhD School of Chemistry, Eötvös Loránd University, Pázmány Péter stny. 1/A, H-1117 Budapest, Hungary
[b] Joint Research and Training Laboratory on Separation Techniques, Institute of Chemistry, Eötvös Loránd University, Pázmány Péter stny. 1/A, H-1117 Budapest, Hungary
[c] Department of Polymer Engineering, Faculty of Mechanical Engineering, Budapest University of Technology and Economics, Műegyetem rkp. 3, H-1111 Budapest, Hungary
[d] ELKH-BME Research Group for Composite Science and Technology, Műegyetem rkp. 3, H-1111 Budapest, Hungary
[e] Department of Methodology for Business Analyses, Faculty of Commerce, Hospitality and Tourism, Budapest Business School, Alkotmány u. 9–11, H-1054 Budapest, Hungary
[f] Wessling International Research and Educational Center, Anonymus u. 6, H-1045 Budapest, Hungary

ARTICLE INFO

Keywords:
Polylactic acid (PLA)
Swelling kinetics
Migration kinetics
Crystallization
Solvent-induced crystallization
Annealing

ABSTRACT

The dependence of swelling and migration on polymer crystallinity was investigated in the case of polylactic acid (PLA)-based plastics. Migration and swelling kinetic experiments were performed at two different temperatures, using plasticized/non-plasticized and annealed/unannealed PLA test specimens. Both swelling and migration proved to be inhibited by the presence of polymer crystals. Crystallization induced clear differences in migration at 40 °C contact temperature, which got more pronounced with the increasing molecular weight (M_w) of additives. At 60 °C the differences diminished, except for Irgafos 168, possibly because of the formation of an inclusion complex type structure. Consequently, to lessen migration, the application of crystallized PLA and high M_w additives in food packaging industry is advantageous. The solvent-induced crystallization of PLA in ethanol 95 *v/v*% was also confirmed, therefore this alternative food simulant should be used with restrictions in the migration testing of PLA-based plastics.

1. Introduction

Polylactic acid (PLA) is undoubtedly one of the most popular biomass derived biodegradable polymers, with wide applicability, e.g., in food industry or pharmaceutical manufacturing. PLA, as a raw material bears many advantageous features, i.e., it has higher Young modulus and tensile strength than polypropylene (PP) or acrylonitrile butadiene styrene (ABS) (Tábi et al., 2021). On the other hand, PLA is a brittle polymer with moderate gas barrier properties (Drieskens et al., 2009) and heat deflection temperature (Tábi et al., 2021). For the improvement of its processability and applicability, PLA is often compounded with plasticizers, e.g., natural citrates (Grigale et al., 2010; Labrecque et al., 1997; Ljungberg & Wesslén, 2002; Shirai et al., 2015; Singh et al., 2020) or lactic acid oligomers (Cicogna et al., 2017; Rojas-Lema et al., 2020). Better heat resistance can be achieved with crystallization or with reinforcement of the polymer, (Graupner et al., 2009; Tábi et al., 2013; Akil et al., 2011) or both at the same time.

While the ratio of amorphous phase in the semi-crystalline polymer decreases with crystallization, the ratio of crystalline region (consequently the density of the polymer) increases. In unmodified PLA the weight percent of crystalline material (or degree of crystallinity, X_C%) is usually only a few percent (Drieskens et al., 2009; Tábi et al., 2016), the exact value is influenced by e.g., the polymer's molecular weight and D-lactide content (Tábi et al., 2019; Tsuji et al., 2006). The X_C% of PLA can be increased intentionally with the application of nucleating agents, with stereocomplexation (Bouapao & Tsuji, 2009; Rahman et al., 2009),

* Corresponding author at: Joint Research and Training Laboratory on Separation Techniques, Institute of Chemistry, Eötvös Loránd University, Pázmány Péter stny. 1/A, H-1117 Budapest, Hungary.
E-mail addresses: noemi.petrovics@ekol.chem.elte.hu (N. Petrovics), csaba.kirchkeszner@ekol.chem.elte.hu (C. Kirchkeszner), antonia.patko@ekol.chem.elte.hu (A. Patkó), tabi@pt.bme.hu (T. Tábi), magyar.norbert@uni-bge.hu (N. Magyar), kovacsneszekely.ilona@uni-bge.hu (I. Kovácsné Székely), balint.szabo@ekol.chem.elte.hu (B.S. Szabó), zoltan.nyiri@ekol.chem.elte.hu (Z. Nyiri), zsuzsanna.eke@ttk.elte.hu (Z. Eke).

https://doi.org/10.1016/j.fpsl.2023.101054
Received 3 October 2022; Received in revised form 23 January 2023; Accepted 13 February 2023

in-mould crystallization (Harris & Lee, 2008; Nagarajan et al., 2015) or post-production crystallization, i.e., annealing (Pan et al., 2008; Pölöskei et al., 2020; Tábi et al., 2016, 2010, 2019; Takayama et al., 2011). During annealing the plastic product is kept at a temperature above its glass transition temperature (T_g), which leads to the formation of the preferred crystalline structure. The rate of crystallizing is highly dependent on the temperature. To achieve the maximum of X_C% in PLA containing 0.5% D-lactide 1 h is enough at 80 °C, while at 100 °C the process takes only a few minutes (Tábi et al., 2019). For annealing no additive is necessary, though, it often lead to the deformation of the products. Therefore, the X_C% of PLA is more often modified with nucleating agents.

The amount of crystalline phase in PLA can also change unintentionally, due to physical aging or solvent-induced crystallization (SIC) (Gao et al., 2012; Naga et al., 2011; Sato et al., 2013; Sonchaeng et al., 2020; Tsuji & Sumida, 2000; Udayakumar et al., 2020; Wu et al., 2014). As PLA gets into contact with a solvent (liquid or vapour), whose molecules are capable of diffusing into the polymer phase, the polymer chain mobility increase. Consequently, the chain relaxation and crystallization of the polymer becomes feasible. Such solvents are e.g., acetone, methanol and ethyl-acetate (Naga et al., 2011; Sato et al., 2013; Tsuji & Sumida, 2000), which swell PLA well, without the dissolution of the polymer. During SIC the solvent molecules act as plasticizers in the polymer phase (Naga et al., 2011). The process of SIC and the resulting crystal morphology is determined by the swelling degree (*SD*%) (Gao et al., 2012), but it is independent from the other characteristics of the solvent (Sato et al., 2013). SIC can proceed at a temperature below the T_g of PLA (even at room temperature), and results in a higher X_C% than annealing at the same temperature and storage time (Udayakumar et al., 2020). As a consequence of SIC, the T_g of PLA changes, however, the direction of change depends on the degree of swelling. At low *SD*% the T_g either remains the same (Sato et al., 2013) or increases (Tsuji & Sumida, 2000) (e.g., in the case of ethanol), while high *SD*% causes T_g decrease (Sonchaeng et al., 2020; Tsuji & Sumida, 2000).

Heat resistance improvement is not the only consequence of crystallization that affects the PLA's applicability as a food contact plastic (FCP). With increased crystallinity, the gas permeability of PLA can be significantly improved (Drieskens et al., 2009; Sawada et al., 2010; Shogren, 1997; Tsuji et al., 2006), which unquestionably suppresses the effect of D-lactide content or molecular weight on the barrier properties of the polymer (Tsuji et al., 2006). The results of Shogren (1997) show 2–3 × difference in the water vapour transmission rate of amorphous (X_C% = 0%) and crystallized (X_C%=66%) PLA. The barrier properties are upgraded because the crystalline parts obstruct the diffusion of gas molecules in the polymer phase by blocking their path. This steric hindrance was proved by Sawada et al. (2010), when they inspected the permeability of gases (H_2, O_2, N_2, CO_2, CH_4) through PLA membranes with different X_C%. Besides the crystallinity caused inhibition of diffusion, the presence of rigid amorphous fraction must be considered too. According to the three-phase model (which describes the structure of semi-crystalline polymers), amorphous fraction is not a heterogenous phase, but it can be divided into two sections: the mobile (MAF) and rigid amorphous fraction (RAF). RAF is the boundary between MAF and the crystalline fraction in the polymer phase, with restricted chain segment mobility. The development of RAF is highly dependent on the temperature, where crystallization takes place – i.e., lower temperature results inhibited polymer chain movement, therefore, RAF and crystalline fraction formation happens in parallel (Delpouve et al., 2013). Despite the obstructed chain mobility, the formation of RAF cause dedensification, and increase the free volume of the polymers by creating high number of holes in the polymer matrix (however, the volume of these holes are smaller than the ones in the MAF) (del Río et al., 2010). Sangroniz et al. (2018) examined the transport properties of annealed PLLAs (poly-L-lactic acid), with different amount of RAF. According to their results, the presence of RAF can counterbalance the effect of crystallinity on the CO_2 permeability and the water vapour transmission rate (due to the increased free volume), however, the amount of crystalline fraction is still the major parameter.

The relation of PLA's gas barrier properties and degree of crystallinity has already been excessively examined. Compared to this, the number of studies investigating the dependence of sorption, desorption or migration (of liquids or plastic additives) on the crystallinity of a polymer is quite limited. Regarding PLA, Tsai et al. (2016) investigated the sorption and desorption behaviour of amorphous (X_C% < 2%) and crystalline (X_C% = 43 ± 1%) PLA in water, methanol and ethanol at 37 °C contact temperature. In the sorption experiments the rate of ethanol uptake of amorphous PLA exceeded that of the crystalline PLA. Though, difference in the equilibrium value of mass uptake was not relevant (6.1 *w*% and 5.0 *w*% to the favour of amorphous PLA).

The investigation of crystallinity dependent migration has previously been performed mostly with polyolefins (Alin & Hakkarainen, 2010; Maghsoud et al., 2018; Marcato et al., 2003). These studies all demonstrated the migration decreasing effect of elevated X_C% at different contact temperatures and times, with different food simulants and heating methods. Differences due to crystallinity were significant: in 2 h contact time the full amount of Irgafos 168 antioxidant migrated into isooctane–ethanol (90 *v/v*%) solution from PP–PE random copolymer, while only 33% release was measured from PP homopolymer (Alin & Hakkarainen, 2010). Reduced migration can be explained again with the barrier effects of crystalline parts and transport path blockage. Maghsoud et al. (2018) supplemented this theory with an additional explanation. They supposed that during the plastic manufacturing, the additive molecules (Irganox 1010 in their study) might be entrapped in the crystalline regions, which further decreases their migration into food simulants.

The importance of migration in terms of food safety (i.e., the transfer of different substances from plastic into food) is a widely known issue that led to the regulation of the packaging industry, among others in the European Union (in Commission Regulation (EU) No. 10/2011 (2011)) "*of 14 January 2011 on plastic materials and articles intended to come into contact with food*"). For the standardization of migration tests, in Commission Regulation (EU) No. 10/2011 food simulants and the conditions of migration tests were determined for the substitution of real storage. The regulation declares that migration tests must be performed to mimic the worst foreseeable case of usage. Among the food simulants, ethanol 95 *v/v*% – an alternative of vegetable oil food simulant – is the most severe for PLA (proved by Kirchkeszner et al. (2022)). In specific cases – for the imitation of long-term, i.e., at least 6 months long storage – accelerated test conditions can be applied. For example, 10 days-long contact with the food simulant at 40 °C covers all times of storage at refrigerated or frozen conditions. The most extreme migration test circumstance is 60 °C contact temperature for 10 days. Additionally, in the Commission Regulation (EU) No. 10/2011 it is also declared, that the conditions of accelerated migration tests must not cause any physical change in the plastic (compared to the real contact conditions).

The aim of our work was to reveal the effect of crystallinity of PLA on the migration of additives, as it can substantially influence its application as food contact material by improving the heat resistance of the polymer. Therefore, the swelling and migration kinetics of injection moulded PLA (annealed and unannealed), with different plasticizer contents and contact temperatures were compared. As food simulant, ethanol 95 *v/v*% was used. For the better understanding of the processes, the individual and simultaneous effects of the above-mentioned parameters were investigated, along with the solvent-induced crystallization of unannealed PLA during the experiments.

2. Materials and methods

2.1. Chemicals and materials

For plastic production, a high viscosity, extrusion type polylactic acid (Ingeo™ Biopolymer 2500HP, Natureworks LLC (Minnetonka,

Minnesota, USA), D-lactide content: 0.5%) was used. As plastic additives, the following substances were applied: BHT (2,6-di-*tert*-butyl-4-methylphenol, CAS: 128–37–0, M_w = 220 g/mol), Uvinul 3039 (2-ethylhexyl 2-cyano-3,3-diphenylacrylate, CAS: 6197–30–4, M_w = 361 g/mol), Tinuvin 900 (2-(2*H*-benzotriazol-2-yl)− 4,6-*bis*(1-methyl-1-phenylethyl) phenol, CAS: 70321–86–7, M_w = 447 g/mol), Irgafos 168 (*tris* (2,4-di-*tert*-butylphenyl) phosphite, CAS: 31570–04–4, M_w = 647 g/mol) and TBAC (tributyl acetyl citrate, CAS: 77–90–7, M_w = 402 g/mol). BHT and Irgafos 168 are among the most popular antioxidants (products of Merck Life Science Co., Budapest, Hungary), while Uvinul 3039 and Tinuvin 900 are UV absorbers (BASF Hungary Ltd., Budapest, Hungary). TBAC, a plasticizer was also purchased from Merck Life Science Co. (Budapest, Hungary). All the above-mentioned materials are allowed to be used intentionally in the production of food contact plastics, according to Commission Regulation (EU) No. 10/2011.

For the quantitative analysis of migrating compounds, mirex (perchloropentacyclodecane, CAS: 2385–85–5) was used as an internal standard. As for food simulant, ethanol 95 *v/v*% (CAS: 64–17–5) was used (Thomasker Finechemicals, Budapest, Hungary).

2.2. Production of Plastics and Test Specimens

Detailed process of plastic production can be found in the work of Kirchkeszner et al. (2022) and Petrovics et al. (2022). Briefly: polylactic acid was heated overnight at 80 °C to remove residual water from the polymer pellets. Then PLA was mixed with the above-mentioned additives: L0 marked plastics contained 1 *w*% of each stabilizer-type additive (overall 4 *w*%), while to L5 plastics 5 *w*% TBAC plasticizer was added, along with the 4 × 1 *w*% stabilizers. Via extrusion (for the compoundation of additives), shredding and injection moulding of PLA, plastic sheets of 80 mm × 80 mm × 2 mm dimensions were produced.

The plastic sheets were cut into smaller pieces for the kinetic tests with a table saw. Dimensions of these test specimens were ca. 40 mm × 20 mm × 2 mm, the accurate size of each piece was measured with Vernier callipers (measurement range: 0–200 mm, with 0.01 mm resolution). The weight of the specimens was measured with an analytical balance (measurement range: 0–120 g, with 0.0001 g resolution).

High degree of crystallinity (X_C%) versions of both L0 and L5 test specimens were prepared via annealing, in a Memmert UNE 200 drying oven (Memmert GmbH + Co.KG, Schwabach, Germany), which was set to 80 °C. According to the results of Tábi et al. (2019), for PLA with low D-lactide content 1 h is enough to reach maximum X_C%, therefore our test specimens were stored in the drying oven for 1 h. These annealed plastics were noted as L0-HC and L5-HC (HC = high degree of crystallinity), while the unannealed ones were marked as L0-LC and L5-LC (LC = low degree of crystallinity (before immersion into ethanol 95 *v/v*%)).

2.3. Characterisation of plastics

The injection moulded and annealed test specimens were characterised via differential scanning calorimetric (DSC) measurements (Q2000 by TA Instruments, New Castle, Delaware, USA). Approximately 5 mg portions of plastics were analysed in a linear heat program, which ranged between 0 and 200 °C, with a temperature increase rate of 5 °C/min. For purge gas 4.5 purity nitrogen was applied.

The thermograms provided information about the glass transition temperature (T_g), cold-crystallization temperature (T_{cc}) and enthalpy of cold-crystallization (ΔH_{cc}), melting temperature (T_m) and enthalpy of fusion (ΔH_m) of analysed plastics. Based on these results, the degree of crystallinity (X_C%) could be determined using Eq. (1).

$$X_C\% = \frac{\Delta H_m - \Delta H_{cc}}{\Delta H_f \bullet (1-\alpha)} \bullet 100 \quad (1)$$

In the equation ΔH_f is the enthalpy of fusion of the absolutely crystallized PLA (93.0 J/g (Battegazzore et al., 2011)) and α is the weight fraction of the additives in the plastics.

The estimated amount of mobile and rigid amorphous fraction can be calculated using Eqs. (2) and (3).

$$X_{MAF}\% = \frac{\Delta C_p}{\Delta C_p^0} \bullet 100 \quad (2)$$

$$X_{RAF}\% = 100 - (X_{MAF}\% + X_C\%) \quad (3)$$

Where X_{MAF}% and X_{RAF}% are the degree of mobile and rigid amorphous fractions, respectively; ΔC_p is the heat capacity step at the glass transition and ΔC_p^0 is the heat capacity step at the glass transition of the fully amorphous PLA (0.48 $J \cdot g^{-1} \cdot K^{-1}$ (Delpouve et al., 2011)). The ΔC_p values were determined based on the work of Delpouve et al. (2011), i.e., with the subtraction of the straight lines fitted to the glassy and liquid-like state parts of the thermograms. However, the X_{MAF}% and X_{RAF}% are usually determined via modulated temperature DSC, an approximation can be calculated from traditional DSC measurements too. The reason of uncertainty (especially in the case of PLA) is the enthalpy recovery and T_g transition overlap, resulting systematic error in the determination of heat capacity change. However, these approximations still can give information on the trends of changing.

DSC analysis of each plastic was performed without any contact with ethanol 95 *v/v*%. In the case of L0-LC and L5-LC plastics, – so that their X_C% and X_{RAF}% change could be characterized during storage in contact with food simulant – further DSC measurements were performed at given times of the kinetic experiments (for the details see Table S2). For these measurements, separate samples were prepared. Each analysis was performed in triplicate.

2.4. Swelling and migration kinetic measurements

The alternative of D2 food simulant (vegetable oil with less than 1% unsaponifiable matter), i.e., ethanol 95 *v/v*% was used in the experiments to achieve reasonable migration in the case of all additives. In the swelling and migration tests, the 40 × 20 × 2 mm test specimens were immersed into ethanol 95 *v/v*% for 15 days. (To meet the 0.6 cm^2/g plastic surface – food simulant mass ratio (as specified in Commission Regulation (EU) No. 10/2011), 6 pieces of test specimens (cc. 110 cm^2 overall surface) were immersed into 230 mL, preheated (40 or 60 °C) ethanol 95 *v/v*%. The sample bottles were then immediately returned to a laboratory incubator (POL-EKO ST2, Pol-Eko-Aparatura, Wodzisław Śląski, Poland). For the quantitative analysis of plastic additives, 200 μL aliquots of samples were taken at the following times: 5 and 30 min; 1, 2, 6 and 12 h; then daily till 15 days. On these occasions the weight of test specimens was also measured with an analytical balance for adjusted swelling degree determination. Each experiment was performed in 5 replicates.

2.5. Quantitative analysis of migrated additives

For the quantitative analysis of the five target compounds, a gas chromatographic – mass spectrometric (GC-MS) method was developed, and its analytical performance characteristics were evaluated by Petrovics et al. (2022). The summary of the GC-MS analytical method can also be found in Table S1.

2.6. Evaluation of data

2.6.1. Calculation of adjusted swelling degree

Adjusted swelling degree (*ASD*%) was introduced by Kirchkeszner et al. (2022), to take the mass changes due to migration into consideration. Our experiences show, that the difference between *ASD*% and swelling degree can be 4.6% (it was measured after 15 days contact time, in the case of L5-LC sample at 60 °C contact temperature). It is to be calculated according to Eq. (4).

$$ASD\% = \frac{(m_{\text{swelled}} + \sum_i c_{V,\text{mig,i}} \bullet V_{\text{simulant}}) - m_{\text{dry}}}{m_{\text{dry}}} \bullet 100 \quad (4)$$

Where m_{swelled} and m_{dry} are the weight of plastic test specimens after and before storage, respectively; $c_{V,\text{mig,i}}$ is the i additive's migrated concentration referred to the volume of food simulant; and V_{simulant} is the volume of food simulant. *ASD*% of each kinetic point was determined from 5 replicates.

Swelling kinetic curves represent the change of *ASD*% over contact time. The final plateau part of kinetic curves (starting at the last range determined with the empirical semivariogram) were characterized with $ASD\%_{\text{max}}$, the arithmetic mean of *ASD*% values. In those cases when range determination was impossible, the results of 13–15 days were averaged (15 datapoints overall).

2.6.2. Calculation of surface normalized concentration

Surface normalized concentration ($c_{A,\text{mig,i}}$) of i migrated additive was calculated from $c_{V,\text{mig,i}}$ so that the results are independent of the small changes of the exact surface of test specimens (A_{specimen}). Eq. (5) gives the formula for this calculation.

$$c_{A,\text{mig,i}} = \frac{c_{V,\text{mig,i}} \bullet V_{\text{simulant}}}{A_{\text{specimen}}} \quad (5)$$

In migration kinetic curves $c_{A,\text{mig,i}}$ results were plotted as a function of contact time. For the determination of $c_{A,\text{mig,i,max}}$ the same process was followed as in the case of $ASD\%_{\text{max}}$.

2.6.3. Swelling and migration rate

Kinetic curves are mostly characterized with the diffusion and partition coefficients, however, for their determination the investigated process must reach its equilibrium. When it does not happen, the dynamic ranges of kinetic curves can be characterized with the swelling and migration rates (Petrovics et al., 2022). For their determination, *ASD*% and $c_{A,\text{mig,i}}$ values were plotted as the function of square root of contact time. According to Crank (1975), the initial part of the transformed function is linear. The slope of this line gives information about the pace of swelling and migration, and these values are referred to as swelling and migration rates, respectively. For the linear fitting the points before the last empirical semivariographic range were used.

2.7. Statistical analysis

2.7.1. Empirical semivariograms

The temporal and spatial autocorrelation of observations can be analysed by a basic function of geostatistics, the so called semivariogram (Hatvani et al., 2021). The method is described in details in the study of Kovács et al. (2012). Numerous research works have been conducted in which variography was successfully applied. Hatvani et al., (2018, 2021) and Trásy et al. (2018) used semivariograms for the recalibration of hydrological monitoring networks. Garamhegyi et al. (2020) and Hatvani et al. (2014) analysed the spatial autocorrelation of the level and the quality of shallow groundwater.

Bodai et al. (2015), Kirchkeszner et al. (2022) and Petrovics et al. (2022) used variography to obtain the necessary contact time to reach a steady-state. Using this method, a range could be determined beyond which the observations were uncorrelated.

If multiple processes affect the variance of the data, more than one range can be obtained, which is indicated by a nested type semivariogram, where the increasing part of the function is followed by variations around more than one constant.

2.7.2. Analysis of variance (ANOVA)

ANOVA was applied to analyse the significant differences between the additives' concentrations and *ASD*% of the given plastic in steady-state. The assumption of normality was verified by Shapiro-Wilk test (Shapiro & Wilk, 1965) which was followed by Bartlett's test (Bartlett, 1937) or Levene's test (Levene, 1960) for the analysis of homogeneity of variance. If the assumptions of ANOVA were not fulfilled, Kruskal-Wallis test (Kruskal & Wallis, 1952) was used followed by Games Howell post-hoc test instead of ANOVA and Tukey test.

2.7.3. Hierarchical cluster analysis (HCA)

The kinetic curves were classified with the use of hierarchical cluster analysis (HCA), Ward method (Ward, 1963) and Euclidean distance to find similarities of migration and swelling processes. Before HCA, the variables were standardized so that the results are not affected by the unit of measure (Magyar et al., 2013).

The following packages of the R software (R Core Team, 2021) were used for the calculation: car, gstat, onewaytests, rstatix, sp, and stats packages.

3. Results and discussion

3.1. Crystallinity and thermal properties of plastic samples

3.1.1. Characterization of plastics before storage

Through injection moulding, plastics containing either only 4 stabilizer-type additives (L0-LC) or the same 4 additives together with a plasticizer, TBAC (L5-LC) were obtained. In both plastics' thermograms, cold-crystallization peaks can be seen, which indicates incomplete crystallization during injection moulding. The amount of estimated RAF was negligible initially: our estimation gave only 4% for L0-LC, and 3% for L5-LC. Degree of crystallinity (X_C%) of the two plastics were 18.1 $\pm$ 0.7% and 23.0 $\pm$ 0.5% for the non-plasticized and plasticized test specimens, respectively (Table S2). The difference in X_C% values is the result of plasticization that affects some other thermal properties of L5-LC plastic too. Its glass transition temperature (T_g) and cold-crystallization temperatures (T_{cc}) are lower than that of the non-plasticized ones, while no considerable difference was experienced in the two plastics' melting temperatures (T_m). Right before the melting, an exothermic peak is observable (related to the α' to α recrystallization), which indicates that the less ordered α' type crystals are also formed during injection moulding in both plastics.

High crystallinity plastics were prepared by annealing and marked as L0-HC (with no plasticizer) and L5-HC (with 5 *w*% plasticizer). Degree of crystallinity of the resulting plastics were 48.3 $\pm$ 0.4% and 47.8 $\pm$ 0.9%, respectively (Table S2). Conclusively, the presence or absence of plasticizer caused no difference in the morphology of these two plastics. Due to the annealing, peaks relating to glass transition and cold-crystallization were not noticeable in the thermograms. With increasing crystallinity, the T_{cc} minimally and the ΔH_m considerably diminish, until the cold-crystallisation exotherm disappears. Annealing did not change T_m, also the small exothermic peak of α'–α phase transition remained visible.

3.1.2. Characterization of plastics after storage in contact with food simulant

When PLA is in contact with swelling solvents, its X_C% increases (detailed results are in Fig. 1, Fig S1 and Table S2) due to plasticization of the polymer, as it has been proved in many studies before (e.g., Naga et al. (2011); Sato et al. (2013)). Since L0-LC and L5-LC sheets were semi-crystalline, the process of solvent-induced crystallisation could be detected in their DSC thermograms.

Solvent-induced crystallisation of L0-LC samples at 40 °C storage temperature can be seen in Fig. 1. (and graphically in Fig. S1A). Along with contact time, the degree of crystallinity of the plastic increased (till 44.1 $\pm$ 0.4%), and the crystallization process reached its equilibrium around 10 days. Parallel with the degree of crystallinity, the estimated amount of RAF increased too. This process reached its maximum with one day delay compared to SIC – after 11 days contact with ethanol 95 *v*/*v*%, the estimated X_{RAF}% was around 40%. In the thermograms the

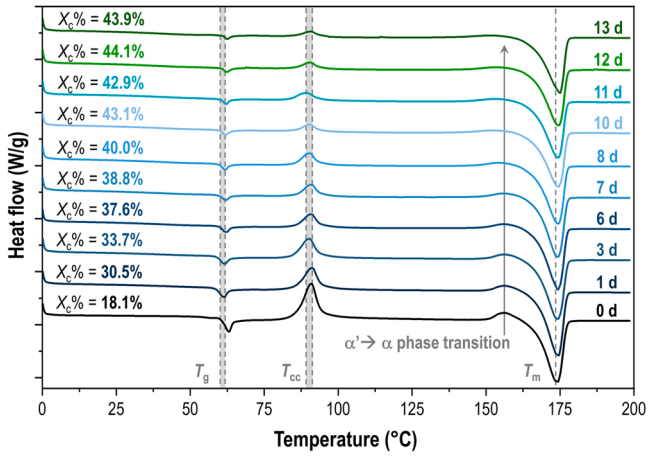

Fig. 1. Changing thermal properties (T_g, T_{cc} and T_m, i.e., glass transition, cold-crystallization and melting temperature, respectively) and degree of crystallinity of L0-LC sample over storage time in ethanol 95 *v/v*% alternative food simulant (determined via differential scanning calorimetry). Curves were shifted vertically with 0.3 W/g to provide better visibility.

cold-crystallization peak decreased with contact time, though it did not disappear completely (similarly to previous reports by e.g., Naga et al. (2011)), and the value of ΔH_{cc} did not change considerably after 10 days storage time (3.8 ± 0.2–5.1 ± 0.2 J/g). In T_g, T_{cc} and T_m no considerable change was noticed. The exothermic peak relating to α'–α phase transition disappeared, so even the perfection of PLA's structure was achieved with SIC.

Plasticized samples (L5-LC) showed similar results at 40 °C contact temperature. With the increasing contact time X_C% and estimated X_{RAF}% grew too, but the process was faster due to the presence of TBAC. Since the presence of TBAC lowered the T_g of PLA, it got closer to the temperature of the experiment, which promoted crystallization. Along with T_g reduction, plasticization also enhances the plastic's swelling (Petrovics et al., 2022), consequently, the solvent-induced crystallization. As a result, only 4 days were necessary to reach the equilibrium of crystallization. The maximum value of X_C% was 44.6 ± 0.3%, which is in good agreement with that of the L0-LC plastic (Table S2). The same can be said about the estimated X_{RAF}%, in the case of L5-LC plastic its amount reached equilibrium at around 40%. The disappearance of α'–α exotherm was also observed. To sum up, TBAC hastened and perfected the crystallization, however, the X_C% value belonging to annealing could not be reached even with plasticization at 40 °C contact temperature.

Contrarily, storage at 60 °C resulted in 47.5 ± 0.8% and 49.5 ± 0.7% degrees of crystallinity (L0-LC and L5-LC, respectively), technically the same as the annealing X_C% values. 60 °C is close to the T_g of both plastics, therefore SIC was fast, and X_C% reached its maximum values in 12 h. With increasing contact time, cold-crystallization exotherms got smaller, by 12 h they completely disappeared. Though, an interesting phenomenon was observable: besides the cold-crystallization peak, a second one appeared in the thermogram of the L5-LC sample after 6 h. Its presence was previously explained by Naga et al. (2011), with the co-existence of an amorphous and a solvent containing, slightly plasticized amorphous phase. The two amorphous phases each have their own cold-crystallization process, each giving their own peak in the thermogram.

3.2. Swelling

3.2.1. Swelling kinetics measured at 40 °C contact temperature

Based on the swelling kinetic curves measured at 40 °C, it can be stated that both plasticizer content and the degree of crystallinity have major effect on the swelling properties of the plastics. As expected, plasticization promoted the swelling, while higher crystallinity hindered it. This resulted in significantly different swelling kinetic curves and *ASD* $\%_{max}$ values ($p = 0.05$) for the four examined plastics (Fig. 2A, C and Table S3).

Comparison of the swelling kinetic curves of samples with the same plasticizer content (L0-LC vs. L0-HC and L5-LC vs. L5-HC) indisputably proved the swelling inhibiting effect of the more arranged – crystallized – structure. The *ASD*$\%_{max}$ values of unplasticized samples reduced from 3.17 ± 0.15% to 1.34 ± 0.21% due to the annealing (L0-LC and L0-HC, respectively). With plasticizer, however, the swelling-inhibiting effect was restrained, and the *ASD*$\%_{max}$ of L5-LC and L5-HC plastics were 6.02 ± 0.20% and 5.22 ± 0.06%, respectively. Though the 5 *w*% TBAC lowered the differentiating effect of crystallinity, the differences in *ASD* $\%_{max}$ remained significant ($p = 0.05$) in all cases. The results of swelling rate showed the same pattern. In case of non-plasticized samples, the swelling of semi-crystalline sample was 2.7 times faster than that of the annealed. This reduced to a 1.5 times difference in plasticizer containing plastics. It is easy to see, that this behaviour is the result of two overlapping effects: high degree of crystallinity inhibits the swelling, but plasticization compensates it.

It is also worth comparing samples of the same crystallinity but different initial plasticizer content (i.e., L0-HC vs. L5-HC and L0-LC vs. L5-LC) (Table S3). The annealed plastics' X_C% were the same at the beginning of migration tests (48.3 ± 0.4% of L0-HC and 47.8 ± 0.9% of L5-HC), but the presence of TBAC caused significant difference in both *ASD*$\%_{max}$ and swelling rate ($p = 0.05$). The swelling rate and *ASD*$\%_{max}$ of L5-HC samples exceeded approximately 4 × the L0-HC samples. The same comparison of semi-crystalline plastics (L0-LC vs. L5-LC) shows smaller – approximately twofold – difference between the plasticized and unplasticized samples. Therefore, apparently, the high X_C% enhanced the differentiating effect of plasticization. The process of annealing is the probable reason for this behaviour: during annealing the arrangement of polymer chains – and crystal region formation – is relatively slow (1 h). This way the additives (or other substances in the polymer matrix) were possibly forced (or "squeezed") out of the newly forming crystalline parts of the polymer and transferred to the amorphous phase or to the surface of the specimen. In the examined annealed plastics (L0-HC and L5-HC with X_C% ~ 48%), the initial weight percent of the amorphous phase was approximately 52%, therefore, TBAC plasticized only that much of the polymer – compared to the unannealed plastics (L0-LC and L5-LC with X_C% ~ 20%) that had circa 80% amorphous phase initially – resulting in an enhanced plasticization.

3.2.2. Swelling kinetics measured at 60 °C contact temperature

Such differences that were previously shown at 40 °C contact temperature in swelling kinetics, were not present at 60 °C. Though the ANOVA analysis indicates significant differences in *ASD*$\%_{max}$ values in some cases ($p = 0.05$), the difference between the highest and lowest *ASD*$\%_{max}$ is only 0.62%. Therefore, the differences might be significant, but can be considered irrelevant (Fig. 2B, D and Table S3).

Instead of the *ASD*$\%_{max}$ values, differences in the swelling kinetic curves are observable in the starting points of steady-states (i.e. ranges determined with empirical semivariography) and swelling rates (Table S3). Ranges clearly indicate the swelling enhancing effect of plasticization and swelling inhibiting effect of annealing. Only 23 h were necessary to reach steady-state in the case of L5-LC sample, while the range of L0-HC sample was 83 h. The L0-LC and L5-HC samples gave closer results, 39 and 46 h, respectively.

For the swelling rate results the same pattern was observable: swelling of the L5-LC was the fastest (1.32 *ASD*%·$h^{-0.5}$) and swelling of the L0-HC was the slowest (0.58 *ASD*%·$h^{-0.5}$) (Table S3). Again, L0-LC and L5-HC gave almost the same results. The reason for the similarity of L0-LC and L5-HC samples is the simultaneous occurrence of a promoting and an inhibiting effect: L0-LC sample did not contain plasticizer, but the initial X_C% was low (18.1 ± 0.7%). Due to the presence of the plasticizer, faster swelling was expected in the case of L5-HC, but the

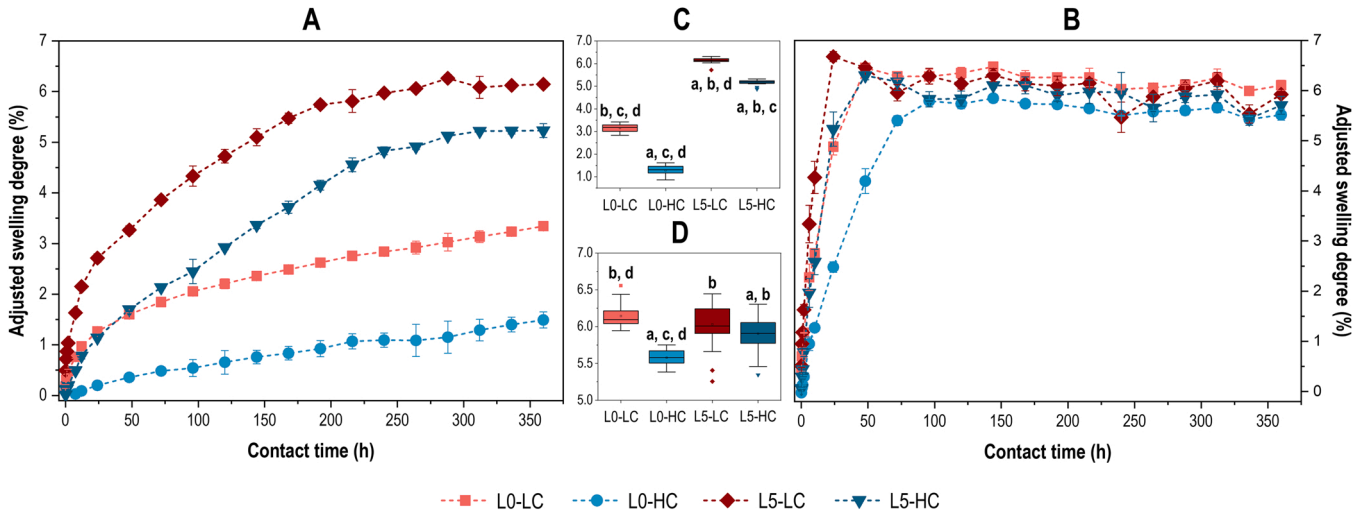

Fig. 2. Adjusted swelling degree kinetic curves (A: 40 °C, B: 60 °C) and the boxplot charts of $ASD\%_{max}$ results (C: 40 °C, D: 60 °C). Letters a–d indicate significant differences ($p = 0.05$) between samples (a: L0-LC, b: L0-HC, c: L5-LC and d: L5-HC). Data represent averages and standard deviations of at least three measurement points with five replicates each.

high $X_C\%$ (47.8 ± 0.9%) obstructed it. Meanwhile, after one day contact time at 60 °C contact temperature, the $X_C\%$ of L0-LC was the same (47.5 ± 0.8%) as that of the L5-HC sample due to solvent-induced crystallization, therefore, the two plastics became indistinguishable regarding both swelling and crystallinity. The fact, that almost no difference was found in the swelling rates (prior the end of SIC) and $ASD\%_{max}$ shows that at high contact temperature (60 °C) the individual effects of plasticization and crystallization can compensate each other. In L0-HC and L5-LC samples, these two effects either absent or occur at the same time, therefore they cannot be concealed by the effect of high contact temperature, and give different results for swelling rate.

3.2.3. *The effect of different contact temperatures on swelling kinetics*

An increase of 20 °C contact temperature has a significant effect on the whole process of swelling, as it can be seen in Table S3 and Fig. 2. Conspicuous differences can be seen in a given plastic's $ASD\%_{max}$ values, in which 1.1–4.4 × growth was observed due to increased temperature (depending on the plasticizer content and $X_C\%$). Those samples were the most affected which contained no plasticizer (L0-LC and L0-HC). The enhancement of swelling decreased due to plasticization until it completely ceased. In the case of L5-LC, $ASD\%_{max}$ values at 40 and 60 °C contact temperatures were the same ($p = 0.05$). Apparently, the maximum swelling degree of 2500HP type PLA is approximately 6.2% in ethanol 95 *v/v*% food simulant, regardless of temperature. It is in harmony with the work of Petrovics et al. (2022), in which the $ASD\%_{max}$ of the same PLA (with 10 *w*% TBAC) at 40 °C contact temperature was 6.54 ± 0.26%. This suggests that the maximum achievable swelling may also be independent of the plasticizer content.

The swelling-enhancing effect of the contact temperature increase is observable in the swelling rates, too. Unplasticized samples produced 5.0 × (L0-LC) and 8.4 × (L0-HC) higher swelling rates at 60 °C. These were reduced to approximately 3 × difference as the result of plasticization.

To compare the mechanism of the whole swelling process of plastics, results were evaluated with hierarchical cluster analysis. The dendrogram shows (Fig. S2) that kinetic curves measured at the same contact temperatures were mostly grouped in one cluster. There is no cluster, in which the swelling results of 40 and 60 °C experiments would be mixed. However, in the case of both temperatures, L0-HC samples were grouped in a separate cluster, while the curves of L0-LC, L5-LC and L5-HC samples shared the same one. This result also confirms the high impact of high $X_C\%$ and lack of plasticizer on the process of swelling.

3.3. *Migration*

3.3.1. *Results of the 40 °C migration tests*

The structural changes in the polymer caused by the swelling in the polymer determine the migration of all kinds of substances from the plastic, which was characterized by the migration tests of four different stabilizer-type additives. Detailed results can be found in Table S4.

The shapes of migration kinetic curves were highly dependent on the test specimens' $X_C\%$. The migrated concentration of additives from annealed plastics changed basically linearly with contact time (R^2 values of a linear fit varied between 0.9683 and 0.9984). As a result, empirical semivariograms were also monotonously increasing, consequently, in the case of L5-HC no range could be identified. Considering the whole time interval the empirical semivariograms of L0-HC also showed increase, but in this case, ranges could be detected. Unannealed samples resulted in nested type empirical semivariograms, i.e., three ranges were found in all cases – around 90, 180 and 260–280 h. The presence of multiple ranges confirms the concurrency of different migration defining parameters.

The maxima of migrated concentrations ($c_{A,mig,i,max}$) show significant differences ($p = 0.05$) between plastic additives in the case of all four plastics (Fig. S3). These results can be explained with the different sizes and molecular weights (M_w) of the examined additives. The maximum migrated concentration is inversely proportional with the M_w of the additives, as it was proved previously by Kirchkeszner et al. (2022). Therefore, the $c_{A,mig,i,max}$ of BHT was the highest (M_w = 220 g/mol), while the one of Irgafos 168 was the lowest (M_w = 646 g/mol) in all cases.

The results of the migration tests show a similar pattern to that of adjusted swelling degree (Section 3.2.1), i.e., the migration of additives from plasticized samples (L5-LC and L5-HC) were the highest. Also, annealed samples showed moderated migration compared to their non-annealed counterparts. The ordered polymer chains with reduced flexibility not only obstructed the solvent uptake, but also blocked the release of substances from the polymer phase. The crystallized regions sterically hindered the migration of additives, and the extent of inhibition depended on the M_w of additives. In Fig. 3. the migration kinetic curves of BHT and Irgafos 168 can be seen, supplemented by the boxplot charts of each additive's $c_{A,mig,i,max}$ results. According to the boxplot charts, the differences in $c_{A,mig,i,max}$ values increase with M_w when the same plasticizer content plastics are compared (L0-LC vs. L0-HC and L5-LC vs. L5-HC). In the case of BHT (M_w = 220 g/mol) and Uvinul 3039 (M_w = 361 g/mol) $c_{A,mig,i,max}$ results were the same from L5-LC and L5-

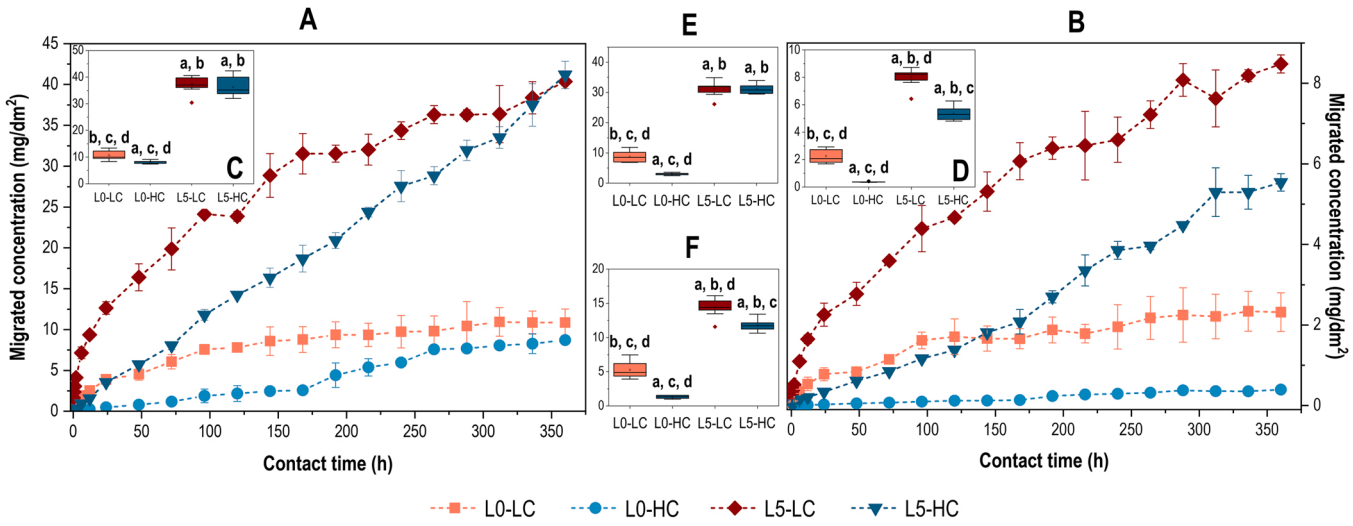

Fig. 3. Migration kinetic curves of BHT (A) and Irgafos 168 (B) additives at 40 °C contact temperature, and the boxplot charts of $c_{A,\mathrm{mig,i,max}}$ results for BHT (C), Irgafos 168 (D), Uvinul 3039 (E) and Tinuvin 900 (F). Letters a–d indicate significant differences ($p = 0.05$) between samples (a: L0-LC, b: L0-HC, c: L5-LC and d: L5-HC). Data represent averages and standard deviations of at least three measurement points with five replicates each.

HC samples (Fig. 3C, E, respectively, and Table S4) ($p = 0.05$), but the differences became significant in the case of Tinuvin 900 ($M_w = 448$ g/mol) and Irgafos 168 ($M_w = 646$ g/mol) (Fig. 3F, D, respectively, and Table S4). The same pattern was observed in the case of non-plasticized plastics; with significant ($p = 0.05$) differences in all cases.

3.3.2. *Results of the 60 °C migration tests*

Even though the increased contact temperature highly influenced the migration kinetics, the differentiating effect of M_w of the additives did not diminish (independently from the plasticizer content or X_C% of the plastic). At 60 °C contact temperature, the starting points of steady-states shifted to lower contact times – and long-lasting steady-states were reached usually within 8 days – yet, differences in $c_{A,\mathrm{mig,i,max}}$ mostly remained significant ($p = 0.05$). It can be seen in Table S4 and the boxplot charts of Fig. S4. In the migration rate results similar trends were observable. The differences between BHT and Uvinul 3039 were small, but the migration rate of Tinuvin 900 was approximately half of that of BHT, and that of Irgafos 168 was even lower. Also, moderate inhibition by crystallized structure was noticeable. Conclusively, M_w not only affects the speed of migration (migration rate), but also determines the achievable maximum of migrated concentration from PLA at 60 °C contact temperature ($c_{A,\mathrm{mig,i,max}}$), if the solubility of additives is not a limiting parameter.

In Fig. 4. the results of migration kinetic tests are plotted (numerical results can be seen in Table S4). According to the boxplot charts only minor differences can be seen in the $c_{A,\mathrm{mig,i,max}}$ results in the case of BHT, Uvinul 3039 and Tinuvin 900 for each plastic, independently from their X_C% and TBAC content. Compared to this, the results of Irgafos 168 are completely different. The maximum migrated concentration of Irgafos 168 was highly dependent on the X_C% of the plastic. ANOVA analysis revealed significant differences ($p = 0.05$) between all plastics, except for L0-LC and L5-LC. As can be seen in Fig. 4B and D, the differences between the two annealed plastics are also negligible. Considering the previous results, this phenomenon is unexpected. For example, at 40 °C contact temperature (Fig. 3) the $c_{A,\mathrm{mig,i,max}}$ results differentiated according to the plastics' plasticizer content (results of L0-LC and L0-HC;

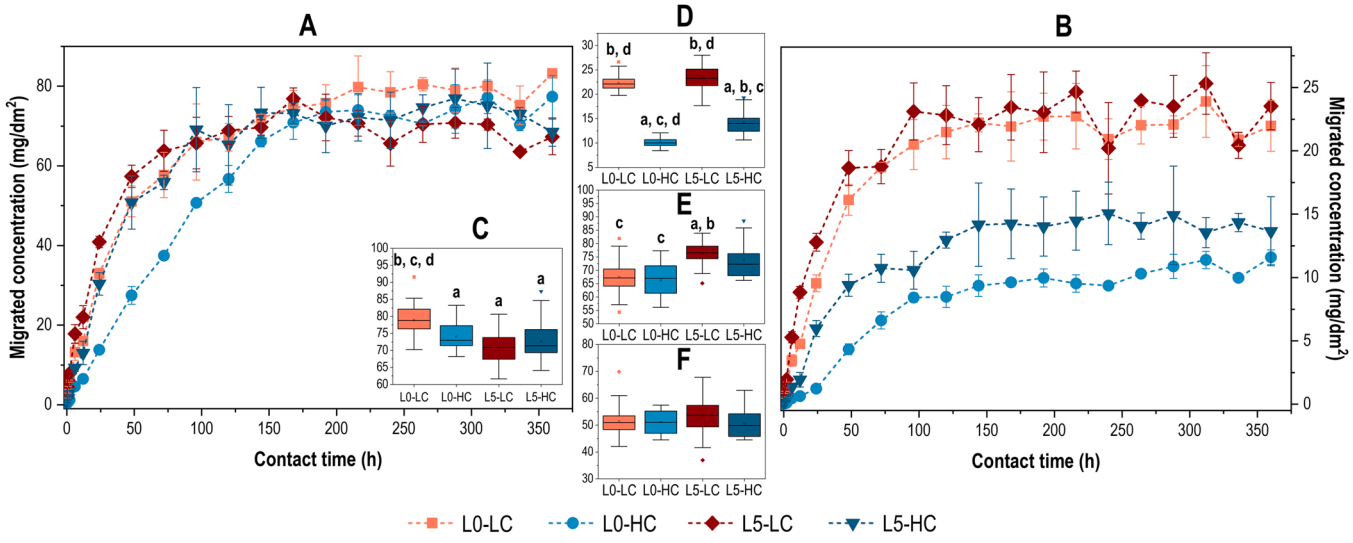

Fig. 4. Migration kinetic curves of BHT (A) and Irgafos 168 (B) additives at 60 °C contact temperature, and the boxplot charts of $c_{A,\mathrm{mig,i,max}}$ results for BHT (C), Irgafos 168 (D), Uvinul 3039 (E) and Tinuvin 900 (F). Letters a–d indicate significant differences ($p = 0.05$) between samples (a: L0-LC, b: L0-HC, c: L5-LC and d: L5-HC). Data represent averages and standard deviations of at least three measurement points with five replicates each.

L5-LC and L5-HC were similar), and X_C% had moderate influence on the results. Long-lasting steady-states were not reached in those experiments. Compared to that, in the case of Irgafos 168 migration at 60 °C, the $c_{A,mig,i,max}$ is clearly determined by the X_C% of plastics (steady-states were reached by 135 h). The anomalous behaviour of Irgafos 168 can be explained with the process of crystal formation during annealing. As the more ordered fraction was forming, the additives were forced out to the amorphous phase (where migration takes place). The results of Irgafos 168 suggest that the excretion is not complete, and partly the additive was incorporated in the newly formed crystals. This structure is probably a kind of inclusion complex, similarly to the ones mentioned by Tsai et al. (2016). Supposedly, during SIC the additive trapping is negligible since the complete process takes at least 12 h. Therefore, complete additive excretion can be assumed. The fact that incorporation was noticeable only in the case of Irgafos 168 (the stabilizer with the highest M_w) suggests that the effectiveness of trapping depends on the size of molecules. The supposed process of migration (and swelling) is illustrated and summarized in Fig. 5.

The migration rates of the additives at 60 °C contact temperature can be found in Table S4. The migration of BHT, Uvinul 3039 and Tinuvin 900 were undoubtedly inhibited from L0-HC plastic, as the result of simultaneous annealing and lack of plasticization. The migration rate results of Irgafos 168 are similar to the $c_{A,mig,i,max}$ results: the migration rates from unannealed L0-LC and L5-LC plastics were similar, while the ones from L0-HC and L5-HC were considerably lower. The migration rate from L0-HC is approximately half of that of L5-HC. This result shows that migration from the non-plasticized plastic is substantially slower, though, $c_{A,mig,i,max}$ reaches similar value in 135 h as in the case of the plasticized sample. Conclusively, with plasticization the migration of Irgafos 168 can be slowed or fastened, but its final migrated concentration is dependent on the crystalline ratio of PLA.

3.3.3. Comparison of migration kinetics at 40 and 60 °C contact temperatures

A change of 20 °C in contact temperature significantly influenced the migration kinetics of the investigated plastic additives. The necessary time to reach steady-states considerably decreased, from 259 to 302 h to 86–286 h. Likewise, the differences in migration rates and the maxima of migrated concentrations are unquestionable (Table S4). Considering any additive – polymer systems, both $c_{A,mig,i,max}$ and migration rate results at 60 °C are several times higher than those at 40 °C. The smallest differences can be found in the case of L5-LC plastic, at which only 2–4 × higher $c_{A,mig,i,max}$ values were measured. The biggest differences were found in the migration from L0-HC plastic (9–40 ×). Based on these results, the 20 °C difference in contact temperature results insurmountable differences in $c_{A,mig,i,max}$, no matter how long the migration is followed.

As it can be seen in Figs. 3 and 4, the shape of migration kinetic curves changed as a result of varying storage conditions, plasticizer content and degree of crystallinity. For the comparison of curves' shapes – and therefore the mechanism of migration – the kinetic curves were analysed with hierarchical cluster analysis (HCA), the result of the analysis is shown in the dendrogram of Fig. S2. Based on it, the mechanism of migration is determined by contact temperature, since most clusters include kinetic curves measured at the same temperature (except for *cluster 6*). The results of 40 °C storage was grouped to *clusters 4* and *7*, while 60 °C curves can be found in *clusters 1*, *2* and *5* (along with *cluster 3*, which contained only *ASD*% curves). The kinetic curves measured at 40 °C were split into two clusters, based on the crystallinity of the plastics: annealed samples (L0-HC and L5-HC) are in *cluster 4*, unannealed samples (L0-LC and L5-LC) can be found in *cluster 7*. The crystallinity-based classification of the 40 °C results was expectable since the original kinetic curves had very different shapes, too. The unannealed plastics produced the expected saturation-shape curves, but

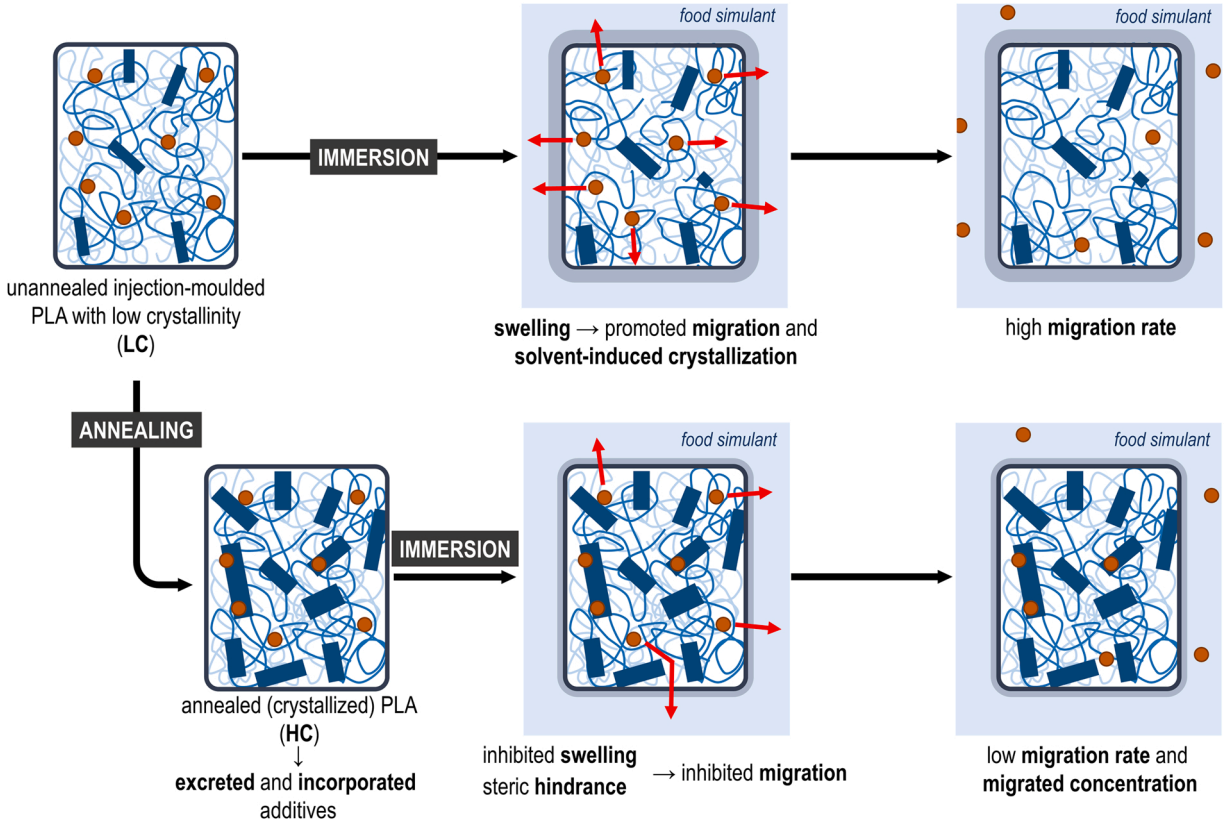

Fig. 5. Supposed scheme for the swelling and migration mechanism of unannealed (upper row) and annealed PLA (lower row), where rectangles and circles represent the crystalline regions and plastic additives, respectively.

the migrated concentration from annealed plastics changed linearly with contact time. This proves that the migration kinetics from the two crystalline ratio plastics are different, which is independent of the physical-chemical properties of additives.

In the case of 60 °C contact temperature, the classification is not as obvious, as even the measured migration kinetic curves bear quite similar shapes (see in Fig. 4.). In cluster grouping the competing effect of plasticization and crystallinity was decisive. In *cluster 2*, the results of L5-LC plastic were grouped, where both TBAC presence and lack of annealing promoted migration. *Cluster 1* is a mixed cluster of L0-LC and L5-HC samples. Similarity of these kinetic curves is the result of concurrent presence of a migration inhibiting and promoting effect, as it was mentioned in Sections 3.2.1 and 3.3.1.

Considering the contact temperature, *cluster 6* is mixed, as it contains all types of plastics' kinetic curves from both 40 and 60 °C migration experiments. Though, the classification was not random. Kinetic curves of L0-LC and L5-LC plastics stored at 40 °C were grouped in this cluster, along with some L0-HC and L5-HC curves of 60 °C contact temperature. According to this result, the mechanism of migration can show similarity between lower temperature storage of more amorphous plastics, and annealed plastics, which were stored at an elevated temperature. It demonstrates that the effect of increasing contact temperature and decreasing crystallinity on the migration of additives can be similar. Though, it must be highlighted again that $c_{A,\mathrm{mig,i,max}}$ and migration rate results were significantly different, cluster analysis provides information only about the similarities (or dissimilarities) of migration mechanism changing circumstances.

4. Conclusions

Swelling and migration kinetic testing of polylactic acid-based plastics with different plasticizer content (0 and 5 *w*%) and initial crystallinity ($X_C\% = 18.1 \pm 0.7$–$48.3 \pm 0.4\%$), at 40 and 60 °C contact temperatures were performed. Thermal characteristics of plastics were followed with differential scanning calorimetric analysis, prior to and during the kinetic measurements. Our results proved the swelling and migration decreasing effect of crystallized structure of PLA. This was investigated in the context of plasticizer content and contact temperature. The summary of concurrent processes can be seen in Fig. 5.

From the aspect of regulatory migration tests, the results of DSC measurements are significant. According to them, the concurrent application of elevated temperature and a polymer swelling food simulant in migration tests, cause the polymer's solvent induced crystallization. Crystallization is noticeable even after a few hours contact at both 40 and 60 °C temperatures. Since it is declared in Commission Regulation (EU) No. 10/2011 that testing conditions must not cause any physical change in test specimens (compared to the real storage), the applicability of ethanol 95 *v/v*% as alternative food simulant for PLA should be restricted. When PLA is crystallized to the maximum achievable $X_C\%$, such limitation is unnecessary though.

Based on our results, we could conclude that plasticization is crucial regarding the rate of swelling and migration, but do not influence relevantly the $ASD\%_{\max}$ or $c_{A,\mathrm{mig,i,max}}$, when long-lasting steady-states were reached. Contrarily, both temperature and degree of crystallinity can be definitive in terms of all above-mentioned parameters. The effect of annealed structure on $c_{A,\mathrm{mig,i,max}}$ could only be observed in the case of the highest M_w additive (Irgafos 168), which means that the size of the migrating substance is also crucial. This result can be important in FCM production: if high M_w stabilizers are applied, and the crystallinity of PLA is set by post-production annealing, the possible additive migration can be significantly reduced, even at high contact temperature and long contact time.

CRediT authorship contribution statement

Noémi Petrovics: Conceptualization, Design and conduct the experiments, Data evaluation and visualization, Formal analysis, Writing – original draft. **Csaba Kirchkeszner:** Writing – review & editing, Conceptualization. **Antónia Patkó:** Conduct the experiments, Data evaluation, Writing – review & editing. **Tamás Tábi:** Production and analysis of plastics, Data interpretation, Writing – review & editing, Funding acquisition. **Norbert Magyar:** Data visualization, Formal analysis, Writing – review & editing. **Ilona Kovácsné Székely:** Data visualization, Formal analysis, Writing – review & editing. **Bálint Sámuel Szabó:** Writing – review & editing, Conceptualization. **Zoltán Nyiri:** Writing – review & editing, Conceptualization. **Zsuzsanna Eke:** Conceptualization, Supervision, Writing – review & editing, Funding acquisition.

Conflict of interest

Declare that they have no conflict of interest.

Data availability

Data will be made available on request.

Acknowledgement

We are thankful to Wessling International Research and Educational Center (WIREC) for providing financial support, laboratory equipment, and materials for our research. The authors gratefully acknowledge the technician staff of Budapest University of Technology and Economics, Faculty of Mechanical Engineering, Department of Polymer Engineering for the help in manufacturing plastic specimens. We are also thankful to BASF Hungary Ltd. for donating Uvinul 3039 and Tinuvin 900 plastic additives. This research program has been implemented with support provided by the National Research, Development and Innovation Fund of Hungary, financed under project No. 128440 of the FK18 funding scheme. This work was also supported by the National Research, Development and Innovation Office, Hungary (2019–1.1.1-PIACI-KFI-2019–00205, 2019–1.1.1-PIACI-KFI-2019–00335, OTKA FK134336). The research reported in this paper has been supported by the NRDI Fund (TKP2020 NC, Grant No. BME-NCS) based on the charter of bolster issued by the NRDI Office under the auspices of the Ministry for Innovation and Technology. This paper was supported by the János Bolyai Research Scholarship of the Hungarian Academy of Sciences. The research was supported by the ÚNKP-21–5 New National Excellence Program of the Ministry for Innovation and Technology from the source of the National Research, Development and Innovation Fund.

Appendix A. Supporting information

Supplementary data associated with this article can be found in the online version at doi:10.1016/j.fpsl.2023.101054.

References

Akil, H. M., Omar, M. F., Mazuki, A. A. M., Safiee, S., Ishak, Z. A. M., & Abu Bakar, A. (2011). Kenaf fiber reinforced composites: A review. *Materials and Design* (Vol. 32, (Issues 8–9), 4107–4121. https://doi.org/10.1016/j.matdes.2011.04.008

Alin, J., & Hakkarainen, M. (2010). Type of polypropylene material significantly influences the migration of antioxidants from polymer packaging to food simulants during microwave heating. *Journal of Applied Polymer Science, 118*(2), 1084–1093. https://doi.org/10.1002/app.32472

Bartlett, M.S. (1937). Properties of Sufficiency and Statistical Tests. Proceedings of the Royal Statistical Society, Series A, 160, 268–282. https://royalsocietypublishing.org/.

Battegazzore, D., Bocchini, S., & Frache, A. (2011). Crystallization kinetics of poly(lactic acid)-talc composites. *Express Polymer Letters, 5*(10), 849–858. https://doi.org/10.3144/expresspolymlett.2011.84

Bodai, Z., Kirchkeszner, C., Novák, M., Nyiri, Z., Kovács, J., Magyar, N., Iván, B., Rikker, T., & Eke, Z. (2015). Migration of Tinuvin P and Irganox 3114 into milk and the corresponding authorised food simulant. *Food Additives and Contaminants - Part A Chemistry, Analysis, Control, Exposure and Risk Assessment, 32*(8), 1358–1366. https://doi.org/10.1080/19440049.2015.1055523

Bouapao, L., & Tsuji, H. (2009). Stereocomplex crystallization and spherulite growth of low molecular weight poly-(l-lactide) and poly(d-lactide) from the melt. *Macromolecular Chemistry and Physics, 210*(12), 993–1002. https://doi.org/10.1002/macp.200900017

Cicogna, F., Coiai, S., de Monte, C., Spiniello, R., Fiori, S., Franceschi, M., Braca, F., Cinelli, P., Fehri, S. M. K., Lazzeri, A., Oberhauser, W., & Passaglia, E. (2017). Poly (lactic acid) plasticized with low-molecular-weight polyesters: structural, thermal and biodegradability features. *Polymer International, 66*(6), 761–769. https://doi.org/10.1002/pi.5356

Commission Regulation (EU) No 10/2011, 2011, of 14 January 2011 on plastic materials and articles intended to come into contact with food. Official Journal of the European Union, 77.

Crank, J., 1975, Some calculated results for variable diffusion coefficient, Non-Fickian diffusion. In Crank, J. The mathematics of diffusion (pp. 160–203, 254–265). Oxford University Press.

del Río, J., Etxeberria, A., López-Rodríguez, N., Lizundia, E., & Sarasua, J. R. (2010). A PALS contribution to the supramolecular structure of poly(l -lactide). *Macromolecules, 43*(10), 4698–4707. https://doi.org/10.1021/ma902247y

Delpouve, N., Saiter, A., & Dargent, E. (2011). Cooperativity length evolution during crystallization of poly(lactic acid. *European Polymer Journal, 47*(12), 2414–2423. https://doi.org/10.1016/j.eurpolymj.2011.09.027

Drieskens, M., Peeters, R., Mullens, J., Franco, D., Iemstra, P. J., & Hristova-Bogaerds, D. G. (2009). Structure versus properties relationship of poly(lactic acid). I. effect of crystallinity on barrier properties. *Journal of Polymer Science, Part B: Polymer Physics, 47*(22), 2247–2258. https://doi.org/10.1002/polb.21822

Gao, J., Duan, L., Yang, G., Zhang, Q., Yang, M., & Fu, Q. (2012). Manipulating poly (lactic acid) surface morphology by solvent-induced crystallization. *Applied Surface Science, 261*, 528–535. https://doi.org/10.1016/j.apsusc.2012.08.050

Garamhegyi, T., Hatvani, I. G., Szalai, J., & Kovács, J. (2020). Delineation of hydraulic flow regime areas based on the statistical analysis of semicentennial shallow groundwater table time series. *Water (Switzerland), 12*(3). https://doi.org/10.3390/w12030828

Graupner, N., Herrmann, A. S., & Müssig, J. (2009). Natural and man-made cellulose fibre-reinforced poly(lactic acid) (PLA) composites: An overview about mechanical characteristics and application areas. *Composites Part A: Applied Science and Manufacturing, 40*(6–7), 810–821. https://doi.org/10.1016/j.compositesa.2009.04.003

Grigale, Z., Kalnins, M., Dzene, A., & Tupureina, V. (2010). Biodegradable Plasticized Poly (lactic acid) Films. *Scientific Journal of Rigasch Technical University, 21*, 97–102.

Harris, A. M., & Lee, E. C. (2008). Improving mechanical performance of injection molded PLA by controlling crystallinity. *Journal of Applied Polymer Science, 107*(4), 2246–2255. https://doi.org/10.1002/app.27261

Hatvani, I. G., Kirschner, A. K. T., Farnleitner, A. H., Tanos, P., & Herzig, A. (2018). Hotspots and main drivers of fecal pollution in Neusiedler See, a large shallow lake in Central Europe. *Environmental Science and Pollution Research, 25*(29), 28884–28898. https://doi.org/10.1007/s11356-018-2783-7

Hatvani, I. G., Magyar, N., Zessner, M., Kovács, J., & Blaschke, A. P. (2014). Die Europäische Wasserrahmenrichtlinie: Kann man aus den Grundwassermessdaten mehr Informationen gewinnen? Eine Fallstudie im Seewinkel, Burgenland, Österreich. *Hydrogeology Journal, 22*(4), 779–794. https://doi.org/10.1007/s10040-013-1093-x

Hatvani, I. G., Szatmári, G., Kern, Z., Erdélyi, D., Vreča, P., Kanduč, T., Czuppon, G., Lojen, S., & Kohán, B. (2021). Geostatistical evaluation of the design of the precipitation stable isotope monitoring network for Slovenia and Hungary. *Environment International*, *146*. https://doi.org/10.1016/j.envint.2020.106263

Kirchkeszner, C., Petrovics, N., Tábi, T., Magyar, N., Kovács, J., Szabó, B. S., Nyiri, Z., & Eke, Z. (2022). Swelling as a promoter of migration of plastic additives in the interaction of fatty food simulants with polylactic acid- and polypropylene-based plastics. *Food Control*, *132*. https://doi.org/10.1016/j.foodcont.2021.108354

Kovács, J., Korponai, J., Székely Kovács, I., & Hatvani, I. G. (2012). Introducing sampling frequency estimation using variograms in water research with the example of nutrient loads in the Kis-Balaton Water Protection System (W Hungary. *Ecological Engineering, 42*, 237–243. https://doi.org/10.1016/j.ecoleng.2012.02.004

Kruskal, W. H., & Wallis, W. A. (1952). Use of ranks in one-criterion variance analysis. *Journal of the Americal Statistical Association, 47*, 583–621.

Labrecque, L. v, Kumar, R. A., Davé, V., Gross, R. A., & Mccarthy, S. P. (1997). Citrate Esters as Plasticizers for Poly (lactic acid). *Journal of Applied Polymer Science, 66*, 1507–1513.

Levene, H. (1960). Robust tests for equality of variances. In Ingram O., Harold Hotelling (Eds.), Contributions to Probability and Statistics: Essays in Honor of Harold Hotelling. (pp. 278–292.). Stanford University Press.

Ljungberg, N., & Wesslén, B. (2002). The effects of plasticizers on the dynamic mechanical and thermal properties of poly(lactic acid). *Journal of Applied Polymer Science, 86*(5), 1227–1234. https://doi.org/10.1002/app.11077

Maghsoud, Z., Rafiei, M., & Famili, M. H. N. (2018). Effect of processing method on migration of antioxidant from HDPE packaging into a fatty food simulant in terms of crystallinity. *Packaging Technology and Science, 31*(3), 141–149. https://doi.org/10.1002/pts.2359

Magyar, N., Hatvani, I. G., Székely, I. K., Herzig, A., Dinka, M., & Kovács, J. (2013). Application of multivariate statistical methods in determining spatial changes in water quality in the Austrian part of Neusiedler See. *Ecological Engineering, 55*, 82–92. https://doi.org/10.1016/j.ecoleng.2013.02.005

Marcato, B., Guerra, S., Vianello, M., & Scalia, S. (2003). Migration of antioxidant additives from various polyolefinic plastics into oleaginous vehicles. *International Journal of Pharmaceutics, 257*(1–2), 217–225. https://doi.org/10.1016/S0378-5173(03)00143-1

Naga, N., Yoshida, Y., Inui, M., Noguchi, K., & Murase, S. (2011). Crystallization of amorphous poly(lactic acid) induced by organic solvents. *Journal of Applied Polymer Science, 119*(4), 2058–2064. https://doi.org/10.1002/app.32890

Nagarajan, V., Zhang, K., Misra, M., & Mohanty, A. K. (2015). Overcoming the fundamental challenges in improving the impact strength and crystallinity of PLA biocomposites: Influence of nucleating agent and mold temperature. *ACS Applied Materials and Interfaces, 7*(21), 11203–11214. https://doi.org/10.1021/acsami.5b01145

Pan, P., Zhu, B., Kai, W., Dong, T., & Inoue, Y. (2008). Polymorphic transition in disordered poly(L-lactide) crystals induced by annealing at elevated temperatures. *Macromolecules, 41*(12), 4296–4304. https://doi.org/10.1021/ma800343g

Petrovics, N., Kirchkeszner, C., Tábi, T., Magyar, N., Kovácsné Székely, I., Szabó, B. S., Nyiri, Z., & Eke, Z. (2022). Effect of temperature and plasticizer content of polypropylene and polylactic acid on migration kinetics into isooctane and 95 v/v% ethanol as alternative fatty food simulants. *Food Packaging and Shelf Life*, *33*. https://doi.org/10.1016/j.fpsl.2022.100916

Pölöskei, K., Csézi, G., Hajba, S., & Tábi, T. (2020). Investigation of the thermoformability of various D-Lactide content poly(lactic acid) films by ball burst test. *Polymer Engineering and Science, 60*(6), 1266–1277. https://doi.org/10.1002/pen.25378

Rahman, N., Kawai, T., Matsuba, G., Kanaya, T., Watanabe, H., Okamoto, H., Kato, M., Usuki, A., Matsuda, M., Nakajima, K., & Honma, N. (2009). Effect of polylactide stereocomplex on the crystallization behavior of poly(L-lactic acid. *Macromolecules, 42*(13), 4739–4745. https://doi.org/10.1021/ma900004d

Rojas-Lema, S., Quiles-Carrillo, L., Garcia-Garcia, D., Melendez-Rodriguez, B., Balart, R., & Torres-Giner, S. (2020). Tailoring the properties of thermo-compressed polylactide films for food packaging applications by individual and combined additions of lactic acid oligomer and halloysite nanotubes. *Molecules, 25*(8). https://doi.org/10.3390/molecules25081976

Sangroniz, A., Chaos, A., Iriarte, M., del Río, J., Sarasua, J. R., & Etxeberria, A. (2018). Influence of the Rigid Amorphous Fraction and Crystallinity on Polylactide Transport Properties. *Macromolecules, 51*(11), 3923–3931. https://doi.org/10.1021/acs.macromol.8b00833

Sato, S., Gondo, D., Wada, T., Kanehashi, S., & Nagai, K. (2013). Effects of various liquid organic solvents on solvent-induced crystallization of amorphous poly(lactic acid) film. *Journal of Applied Polymer Science, 129*(3), 1607–1617. https://doi.org/10.1002/app.38833

Sawada, H., Takahashi, Y., Miyata, S., Kanehashi, S., Sato, S., & Nagai, K. (2010). Gas transport properties and crystalline structures of poly(lactic acid). *membranes Transaction of the Materials Research Society of Japan, 35*(2), 241–246.

Shapiro, S. S., & Wilk, M. B. (1965). An Analysis of Variance Test for Normality (Complete Samples). *Biometrika, 52*(3), 591–611. ⟨https://www.jstor.org/stable/2333709⟩.

Shirai, M. A., Müller, C. M. O., Grossmann, M. V. E., & Yamashita, F. (2015). Adipate and Citrate Esters as Plasticizers for Poly(Lactic Acid)/Thermoplastic Starch Sheets. *Journal of Polymers and the Environment, 23*(1), 54–61. https://doi.org/10.1007/s10924-014-0680-9

Shogren, R. (1997). Water Vapor Permeability of Biodegradable Polymers. *Journal of Environmental Polymer Degradation, 5*, 2.

Singh, A. A., Sharma, S., Srivastava, M., & Majumdar, A. (2020). Modulating the properties of polylactic acid for packaging applications using biobased plasticizers and naturally obtained fillers. *International Journal of Biological Macromolecules, 153*, 1165–1175. https://doi.org/10.1016/j.ijbiomac.2019.10.246

Sonchaeng, U., Auras, R., Selke, S., Rubino, M., & Lim, L. T. (2020). In-situ changes of thermo-mechanical properties of poly(lactic acid) film immersed in alcohol solutions. *Polymer Testing*, *82*. https://doi.org/10.1016/j.polymertesting.2019.106320

Tábi, T., Ageyeva, T., & Kovács, J. G. (2021). Improving the ductility and heat deflection temperature of injection molded Poly(lactic acid) products: A comprehensive review. In *In Polymer Testing* (Vol. 101). Elsevier Ltd,. https://doi.org/10.1016/j.polymertesting.2021.107282

Tábi, T., Hajba, S., & Kovács, J. G. (2016). Effect of crystalline forms (α′ and α) of poly (lactic acid) on its mechanical, thermo-mechanical, heat deflection temperature and creep properties. *European Polymer Journal, 82*, 232–243. https://doi.org/10.1016/j.eurpolymj.2016.07.024

Tábi, T., Sajó, I. E., Szabó, F., Luyt, A. S., & Kovács, J. G. (2010). Crystalline structure of annealed polylactic acid and its relation to processing. *Express Polymer Letters, 4*(10), 659–668. https://doi.org/10.3144/expresspolymlett.2010.80

Tábi, T., Tamás, P., & Kovács, J. G. (2013). Chopped basalt fibres: A new perspective in reinforcing poly(lactic acid) to produce injection moulded engineering composites from renewable and natural resources. *Express Polymer Letters, 7*(2), 107–119. https://doi.org/10.3144/expresspolymlett.2013.11

Tábi, T., Wacha, A. F., & Hajba, S. (2019). Effect of D-lactide content of annealed poly (lactic acid) on its thermal, mechanical, heat deflection temperature, and creep properties. *Journal of Applied Polymer Science, 136*(8). https://doi.org/10.1002/app.47103

Takayama, T., Todo, M., & Tsuji, H. (2011). Effect of annealing on the mechanical properties of PLA/PCL and PLA/PCL/LTI polymer blends. *Journal of the Mechanical Behavior of Biomedical Materials, 4*(3), 255–260. https://doi.org/10.1016/j.jmbbm.2010.10.003

Trásy, B., Garamhegyi, T., Laczkó-Dobos, P., Kovács, J., & Hatvani, I. G. (2018). Geostatistical screening of flood events in the groundwater levels of the diverted inner delta of the Danube River: Implications for river bed clogging. *Open Geosciences, 10*(1), 64–78. https://doi.org/10.1515/geo-2018-0006

Tsai, W. C., Hedenqvist, M. S., Laiback, Melin, H., Ngo, M., Trollsås, M., & Gedde, U. W. (2016). Physical changes and sorption/desorption behaviour of amorphous and

semi-crystalline PLLA exposed to water, methanol and ethanol. *European Polymer Journal, 76*, 278–293. https://doi.org/10.1016/j.eurpolymj.2016.02.005

Tsuji, H., Okino, R., Daimon, H., & Fujie, K. (2006). Water vapor permeability of poly (lactide)s: Effects of molecular characteristics and crystallinity. *Journal of Applied Polymer Science, 99*(5), 2245–2252. https://doi.org/10.1002/app.22698

Tsuji, H., & Sumida, K. (2000). Poly(L-lactide): V. Effects of Storage in Swelling Solvents on Physical Properties and Structure of Poly(L-lactide). *Journal of Applied Polymer Science, 79*, 1582–1589.

Udayakumar, M., Kollár, M., Kristály, F., Leskó, M., Szabó, T., Marossy, K., Tasnádi, I., & Németh, Z. (2020). Temperature and time dependence of the solvent-induced crystallization of poly(L-lactide. *Polymers, 12*(5). https://doi.org/10.3390/POLYM12051065

Ward, J. H. (1963). Hierarchical grouping to optimize an objective function. *Journal of the American Statistical Association, 58*(301), 236–244. https://doi.org/10.1080/01621459.1963.10500845

Wu, N., Lang, S., Zhang, H., Ding, M., & Zhang, J. (2014). Solvent-induced crystallization behaviors of PLLA ultrathin films investigated by RAIR spectroscopy and AFM measurements. *Journal of Physical Chemistry B, 118*(44), 12652–12659. https://doi.org/10.1021/jp506840e